First principles investigation of protactinium-based oxide-perovskites for flexible opto–electronic devices

Nazia Erum[1,†] and Muhammad Azhar Iqbal[1,2]

[1] Physics Department, University of the Punjab, Quaid-e-Azam Campus, P. O. Box 54590 Lahore, Pakistan
[2] School of Science, University of Management and Technology, C-ll, Johar Town Campus, P. O. Box 54770 Lahore, Pakistan

(Received 30 November 2016; revised manuscript received 22 December 2016; published online 20 February 2017)

The structural, elastic, mechanical, electronic, and optical properties of $KPaO_3$ and $RbPaO_3$ compounds are investigated from first-principles calculations by using the WIEN2k code in the frame of local density approximation (LDA) and generalized gradient approximation (GGA). The calculated ground state quantities, such as lattice constant (a_0), ground state energy (E), bulk modulus (B), and their pressure derivative (B_p) are in reasonable agreement with the present analytical and previous theoretical results and available experimental data. Based on several elastic and mechanical parameters, the structural stability, hardness, stiffness and the brittle and ductile behaviors are discussed, which reveal that protactinium-based oxide series of perovskites is mechanically stable and possesses weak resistance to shear deformation compared with resistance to unidirectional compression while flexible and covalent behaviors are dominated in them. The analysis of band profile through Trans–Blaha modified Becke–Johnson (TB-mBJ) potential highlights the underestimation of bandgap with traditional density functional theory (DFT) approximation. Specific contribution of electronic states is investigated by means of total and partial density of states and it can be evaluated that both compounds are (Γ–Γ) direct bandgap semiconductors. All fundamental optical properties are analyzed while attention is paid to absorption and reflection spectra to explore extensive absorptions and reflections of these compounds in high frequency regions. The present method represents an influential approach to calculating the whole set of elastic, mechanical, and opto–electronic parameters, which would conduce to the understanding of various physical phenomena and empower the device engineers to implement these materials in flexible opto–electronic applications.

Keywords: first-principles study, oxide perovskites, mechanical property, electronic property, optical property

PACS: 71.15.Mb, 71.22.+i, 71.15.Ap **DOI:** 10.1088/1674-1056/26/4/047102

1. Introduction

The class of compound with the chemical formula ABO_3 is known as perovskite-type oxide. Here A is usually alkali, alkaline or rare earth metals while B is supposed to be transition, post transition, and non-transition metals although anion is represented by X that are oxides and halides.[1–6] Nowadays material scientists are paying attention to fabricating faster, efficient, and flexible opto–electronic devices. Among the perovskite-type oxides, $KPaO_3$, and $RbPaO_3$ which has been reported as an ideal cubic perovskite-type structure,[7] have received considerable attention because of their mechanical flexibility, good optical quality, high catalytic activity, and high melting point. These $XPaO_3$ (X = K, Rb) compounds can possibly be used for fabricating flexible perovskite solar cells for optical pathways,[8] as high-performance broadband photodetectors for color-sensitive photodiodes,[9] as flexible neural recording devices for medical diagnoses,[10] and as liquid crystal displays (LCD), ionic conducting, luminescence capacitor UV detectors as well as light emitting diodes (LED) for integrated devices.[11,12]

From the above literature it is clear that the $XPaO_3$ (X = K, Rb) compounds are technically sound but even then, little scientific work has been reported on them, which motivates us to investigate them in detail. To the best of our knowledge, there has been no computational study on these compounds so far. To address significant properties, in the present work, we investigate structural, elastic, mechanical, electronic, and optical properties of cubic $XPaO_3$ (X = K, Rb) perovskite compounds at ambient pressure by using the *ab-initio* full potential-linearized augmented plane wave (FP-LAPW) method. The rest of this paper is organized as follows. In Section 2, the methods and some computational details of calculations are given. In Section 3, the results and discussion of structural, elastic, mechanical, electronic, and optical properties of $XPaO_3$ (X = K, Rb) compounds are presented. Finally, in Section 4, all results are compared with previous results available and the main conclusions of the work are drawn, which enlighten future prospective research.

2. Method of calculation

The present first principles study is carried out on the basis of density functional theory (DFT) which is implemented in WIEN2k code[13] to solve Kohn–Sham equation[14] within full potential linearized augmented plane wave (FP-LAPW) method[15–17] for appropriately computing the electronic states and optical response of $XPaO_3$ (X = K, Rb) com-

†Corresponding author. E-mail: erum.n@hotmail.com

© 2017 Chinese Physical Society and IOP Publishing Ltd

pounds. For structural optimization and elastic properties, the exchange–correlation approximation is treated with the generalized gradient approximation (GGA)[18] and local density approximation (LDA)[19] while for electronic and optical properties recently bugged GGA plus Trans–Blaha modified Becke–Johnson (TB-mBJ) potential is employed.[20]

In order to enhance accuracy in calculation, valence electrons are treated semi-relativistically and core electrons are treated fully relativistically. Convergence in basis size is achieved with a cut-off $R_{\mathrm{MT}}K_{\max} = 8.5$, which is product of smallest muffin-tin (reduced muffin-tin (RMT)) radius and the largest plane wave vector $K_{\max}$. The Brillouin zone (BZ) integration is done with 56-K point by using the modified form of tetrahedron method.[21] The calculations are self-consistently converged when total energy and charge are stable within 10^{-5} eV respectively. However, the calculation of optical properties requires a dense mesh of uniformly distributed K-points along the Brillouin zone (BZ). In addition to it, accurate values of bulk modulus are calculated by fitting volume versus energy curve within Birch–Murnagahan's equation of state (EOS)[22] and by calculating elastic constants through using Eq. (8) as mentioned in Table 1 and Table 3 respectively.

3. Results and discussion

3.1. Structural properties

Ternary oxide perovskites $KPaO_3$ and $RbPaO_3$ crystallize into ideal cubic structure with space group $Pm3m$ (#221). Figure 1 illustrates the crystal structure and total energy as a function of unit cell volume in which sites of Wyckoff coordinates occupy 1a (0 0 0), 1b (1/2, 1/2, 1/2), 3c (0, 1/2, 1/2) for X (X = K, Rb), Pa and O respectively. In order to calculate structural properties of $XPaO_3$ (X = K, Rb) the energy minimization process is employed, where the total energy (E) and the corresponding equilibrium cell volume (V_0) are calculated by taking a series of different lattice parameters. The calculated equilibrium lattice constant (a_0), ground state energy (E_0), bulk modulus (B_0), and pressure derivative of bulk modulus (B_{P}) by generalized gradient approximation (GGA) as well as local density approximation (LDA) exchange correlation schemes are presented in Table 1.

It can be analyzed from the data that lattice constant of the $KPaO_3$ is smaller than $RbPaO_3$. It can be easily explained by the following relation: $R(\mathrm{K}) = 2.43$ Å $> R(\mathrm{Rb}) = 2.65$ Å. Lattice constants are also calculated by two analytical methods. The first is ionic radius method while the second method is predicted by Verma and Jindal. The first method employs the following formula:[30]

$$a_0 = \alpha + \beta\,(r_X + r_{\mathrm{O}}) + \gamma\lambda\,(r_{\mathrm{Pa}} + r_{\mathrm{O}}), \tag{1}$$

where α (0.06741), β (0.4905), and γ (1.2921) are constants, r_X is the ionic radius of K (1.64 Å) or Rb (1.72 Å), r_{Pa} is the ionic radius of Pa (0.90 Å) and r_{O} is the ionic radius of O (1.35 Å). Verma and Jindal model is based on the number of valence electrons and average ionic radius that uses the following relation[31]

$$a_0 = K(V_X V_{\mathrm{Pa}} V_{\mathrm{O}})^S r_{\mathrm{av}}, \tag{2}$$

where V_X, V_{Pa}, and V_{O} are valence electrons in X, Pa, and O that are 1, 2, and 6 respectively; K (2.45) and S (0.09) are constants for cubic system; r_{av} is the average ionic radius of $XPaO_3$ system. The lattice constants calculated by using Eqs. (2) and (3) are presented in Table 1. The calculated lattice constants via density functional theory (DFT) and I. R methods show deviation within 2%–3% while V. J method shows deviation within 7%–8% which is due to the dependence of Eq. (2) on the number of valence electrons. However, the results from the density functional theories (DFT) and experimental results are found to be consistent with each other. In addition to it we use the lattice parameters calculated by generalized gradient approximation (GGA) for investigating elastic, mechanical, electronic, and optical properties. The value of bulk modulus represents good crystal rigidity.[32,33] From Table 1 it is clear that $KPaO_3$ has a higher value of bulk modulus than $RbPaO_3$ compound. Furthermore, Table 1 depicts contrary relation between lattice constant and bulk modulus to the trend of other perovskite compounds, which are mentioned in Refs. [34] and [35].

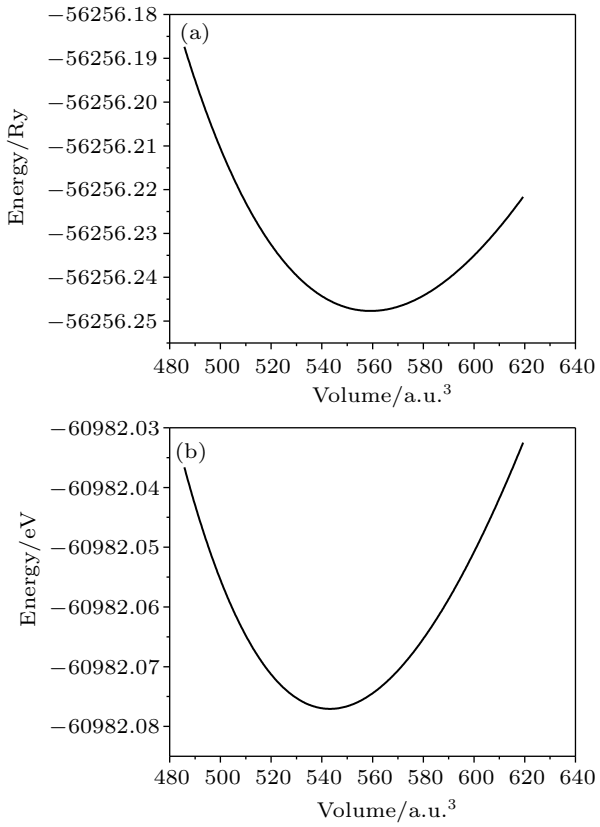


Fig. 1. Variations of the total energy (E, in unit Ry, the unit 1 Ry = 13.6056923(12) eV) with unit cell volume (V, in unit (a.u.)^3) for (a) $KPaO_3$ and (b) $RbPaO_3$.

Table 1. Comparisons of calculated values of the bond length, equilibrium lattice constant (a_0 in unit Å), ground state energy (E_0 in unit Ry), bulk modulus (B_0 in unit GPa), and its pressure derivative (B_P) with experimental and other theoretical results for XPaO$_3$ (X = K, Rb) compounds.

Compound	Present work GGA	Present work LDA	Present analytical work I. R method	Present analytical work V. J methord	Experimental work	Other theoretical work
$KPaO_3$						
a_0/Å	4.37	4.32	4.29	3.99	4.34[a], 4.36[b], 4.38[c]	4.34[d], 4.32[d], 4.18[e], 4.24[f], 4.23[g]
E_0/Ry	−56260.653	−56260.713				
B_0/GPa	203.51	203.63				
B_P/GPa	3.99	3.98				
Bond-lengths						
K–O/Å	2.51					
K–Pa/Å	3.23					
Pa–O/Å	1.81					
$RbPaO_3$						
a_0/Å	4.42	4.35	4.32	4.05	4.37[a], 4.40[b], 4.39[c]	4.36[d], 4.37[d], 4.27[e], 4.26[f], 4.26[g]
E_0/Ry	−60982.210	−60982.279				
B_0/GPa	146.58	146.65				
B_P/GPa	4.122	4.291				
Bond-lengths						
Rb–O/Å	2.61					
Rb–Pa/Å	3.81					
Pa-O/Å	1.82					

[a]Ref. [23], [b]Ref. [24], [c]Ref. [25] (experimental work), [d]Ref. [26], [e]Ref. [27], [f]Ref. [28], [g]Ref. [29] (other theoretical work).

The analyses of chemical trends are performed with the help of chemical bonding where bond length is an average distance between centers of two bonded atoms and which can be used to estimate structural symmetry in terms of tolerance factor. In Table 1 ⟨Pa–O⟩ and ⟨X–O⟩ are the average bond lengths between (Pa, O) and (X, O) atoms respectively. Bond length between X and O increases as K approaches to Rb and this increase is due to lesser size of Rb than that of K compound. A similar trend is observed between bond lengths of Pa and X. The calculated bond lengths can be used to evaluate tolerance factors for $KPaO_3$ and $RbPaO_3$ compounds.[36]

$$t = \frac{0.707\langle X\text{–O}\rangle}{\langle \text{Pa–O}\rangle}, \tag{3}$$

where ⟨X–O⟩ and ⟨Pa–O⟩ represent the average bonds lengths of Pa and O and X (X = K, Rb) and O respectively. The calculated tolerance factors for both perovskites are presented in Table 2, while both compounds satisfy good tolerance factor criterion for cubic perovskites which lies within the range 0.93–1.02.[37]

Table 2. The calculated values of the tolerance factor for XPaO$_3$ (X = K, Rb).

Tolerance factor	Present work Bond length formula	Present work Goldschmidt's formula	Other work
$KPaO_3$	0.985	0.992	0.993[a]
$RbPaO_3$	1.014	1.018	1.019[a]

[a] Ref. [29]

3.2. Elastic properties

Elastic property of solid can play a significant role in explaining the valuable information about the structural stability and the binding characteristic.[38] For a cubic system, there are three independent elastic constants C_{11}, C_{12}, and C_{44} that are summarized in Table 3. Unfortunately, as far as we know for comparison neither experimental nor theoretical values for elastic constants have been available. It is found that all calculated elastic constants fulfill mechanical stability criteria because it cannot be ensured that a particular crystal structure is in a stable or metastable phase unless its elastic constants obey traditional mechanical stability condition at ($P = 0$ GPa), i.e., $C_{11} - C_{12} > 0$, $C_{11} > 0$, $C_{44} > 0$, and $C_{11} + 2C_{12} > 0$ and also satisfy the cubic stability condition, i.e., $C_{12} < B < C_{11}$, which indicates the stabilities of these compounds in cubic phase.[39]

Generally, the C_{11} which reflects resistance to unidirectional compression along the principle crystallographic direction, is higher for $KPaO_3$ and lower for $RbPaO_3$, which confirms that $KPaO_3$ retains weak resistance to unidirectional compression. Similar results of C_{11} are observed in Ref. [40], which agrees well with behaviors of our compounds. Similarly the results of C_{44} indicate that XPaO$_3$ (X = K, Rb) compounds possess higher resistance to the compression than to shear deformation.

3.3. Mechanical properties

Using data of single crystal elastic properties we calculate poly crystalline elastic properties such as Hill's modulus,

Voigt's modulus, Reuss's modulus, Young's modulus, bulk modulus, shear modulus, elastic stiffness coefficients, Poisson's ratio, and melting temperature according to some proposed relationship as mentioned in Ref. [41]. The bulk modulus and shear modulus are equally engaged to measure hardness of material. Here Voigt–Reuss–Hill (VRH) approximation is used to explore shear modulus (G_H) and bulk modulus (B) as follows:[42,43]

$$G_V = \frac{1}{5}(C_{11} - C_{12} + 3C_{44}), \tag{4}$$

$$G_R = \frac{5C_{44}(C_{11} - C_{12})}{4C_{44} + 3(C_{11} - C_{12})}, \tag{5}$$

$$G = \frac{G_V + G_R}{2}. \tag{6}$$

The bulk modulus B can be explained by the following equation:[44]

$$B = \frac{1}{3}(C_{11} + 2C_{12}). \tag{7}$$

From Table 3 it can be observed that for bulk modulus and shear modulus, $RbPaO_3$ has smaller value (146.98 GPa, 69.48 GPa) than $KPaO_3$ (20378 GPa, 70.25 GPa) respectively. In order to define response of a material to linear strain, the empirical formula of Young's modulus is given as follows:[45]

$$y = \frac{9BG}{(3B + G)}. \tag{8}$$

$KPaO_3$ has higher values of Young's modulus Y, bulk modulus B, and shear modulus G, which implies higher sharing of charge transfer among anion and cation than $RbPaO_3$.

Table 3. Calculated values of elastic constants (C_{11}, C_{12}, and C_{44} in GPa) , bulk modulus (B in GPa), Young's modulus (Y in GPa), Voigt's shear modulus (G_V in GPa), Reuss's shear modulus (G_R in GPa), Hill's shear modulus (G_H in GPa), and B/G ratio for $XPaO_3$ (X = K, Rb) compounds.

Sr. No.	Parameters	$KPaO_3$	$RbPaO_3$
1	C_{11}	432.182	311.413
2	C_{12}	89.586	64.767
3	C_{44}	34.816	46.377
4	B_0	203.785	146.982
5	G_v	89.408	77.155
6	G_R	51.101	61.802
7	G_H	70.254	69.478
8	Y	189.038	180.06
9	B_0/G_H	2.901	2.120

Pugh's index of ductility (B/G), Cauchy's pressure, and Poisson's ratio (v) are the factors, which give information about flexible/brittle nature of a material. Pugh's B/G ratio is related to resistance to plastic deformation. Value of $B/G < 1.75$ refers to the brittle material, while $B/G > 1.75$ the ductile or flexible material.[46] Our compounds fulfill the second criterion of B/G ratio (as mentioned above) which depicts strong ductile or flexible nature of $XPaO_3$ compound.

The Cauchy's pressure is defined as the difference between the two particular elastic constants and serves as an indication of flexibility. If the pressure is positive (negative), the material is expected to be flexible (brittle).[47,48]

$$C'' = C_{12} - C_{44}. \tag{9}$$

$B/G > 1.75$ and Cauchy's pressure $C'' > 0$ for both compounds imply that each of them is flexible and contains high directional bonding. Poisson's ratio (v) delivers the information about the flexibility characteristics via the following equation:[49]

$$v = \frac{(3B - 2G)}{2(3B + G)}. \tag{10}$$

According to Frantsevich *et al.*,[50] the critical value of material is 0.26. If the Poisson's ratio is less than 0.26 then the material will be brittle otherwise the material will be flexible. With reference to all the above literature $XPaO_3$ (X = K, Rb) compounds possess dominant flexible nature.

Another parameter is shear constant that can be defined as follows:[51,52]

$$C' = \frac{1}{2}(C_{11} - C_{12}). \tag{11}$$

In fact, the covalent compounds have high values of shear constant. Under investigation, compounds have high values of shear constant, which confirms covalent behaviors in these compounds.

In manufacturing disciplines, the elastic anisotropy parameter A plays a vital role. It is expressed as[53]

$$A = \frac{2C_{44}}{(C_{11} - C_{12})}. \tag{12}$$

The crystal is characterized as being completely isotropic if the value of A is equal to 1. Table 4 shows that the calculated elastic anisotropic factor deviates from unity, which indicates that none of these compounds are elastically isotropic. In addition, based on the empirical formula[54] the melting temperature T_m of $KPaO_3$ shows higher tendency than $RbPaO_3$ compound.

$$T_m = 607 + 9.3B + 555. \tag{13}$$

Table 4. Calculated values of shear constant (C'), Cauchy pressure (C''), Lame's coefficients (λ and μ), Kleinman parameter (ξ in GPa), anisotropy constant (A in GPa), Poisson's ratio (v in GPa), and the melting temperature (T_m in K) for $XPaO_3$ (X = K, Rb) compounds.

Sr. No.	Parameters	$KPaO_3$	$RbPaO_3$
1	C'	171.29	123.32
2	C''	54.77	18.39
3	v/GPa	0.35	0.30
4	A/GPa	0.20	0.38
5	ξ/GPa	0.36	0.36
6	λ	156.77	100.04
7	μ	70.27	69.52
8	T_m/K	3057	2529

3.4. Electronic structure and density of states (DOS)

The electronic properties of protactinium-based oxide perovskite compounds are described by calculating energy band structure and total and partial density of states (TDOS and PDOS) whereas bonding nature is evaluated by the electron density plots through using Trans–Blaha modified Becke–Johnson (TB-mBJ).[55] The bandgap is compared with those from other density functional theory (DFT) exchange and correlation schemes as shown in Table 5. The calculated band structures along highly symmetric directions in the Brillouin zone (BZ) are shown in Fig. 2. At zero pressure, these compounds reveal (Γ–Γ) direct bandgaps of 3.60 eV and 3.14 eV for $KPaO_3$ and $RbPaO_3$ compounds respectively. Unfortunately, there is a lack of experimental data to make a reasonable comparison. However, these compounds can work well in the ultraviolet (UV) region of the electromagnetic spectrum because the material with a bandgap larger than 3.1 eV can work well in the ultraviolet region of the electromagnetic spectrum.[56]

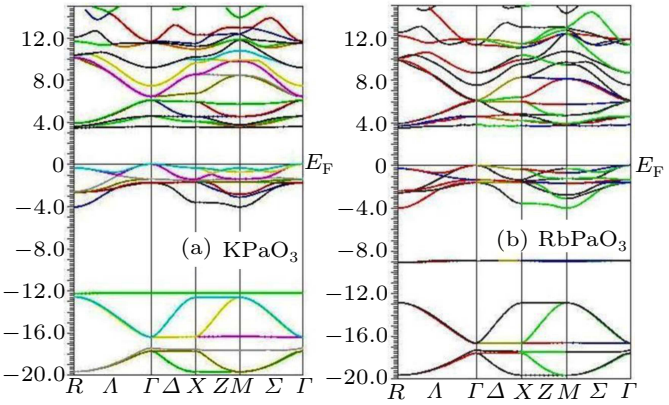


Fig. 2. (color online) Electronic energy dispersion curves for (a) $KPaO_3$ and (b) $RbPaO_3$ along some high symmetry directions in the Brillouin zone (BZ) within modified Becke–Johnson potential.

The number of available states (to occupy) at each energy level is observed in terms of total and partial density of states (TDOS & PDOS). The density of states (DOS) in Fig. 3 occupies energy intervals from ($E_F - 20$ eV) up to ($E_F + 15$ eV). A narrow sharp peak is observed at ($E_F - 20$ eV) due to the presence of O-2s states. Next energy interval ($E_F - 15$ eV) is dominated by Pa-5p states. The upper valence band situated in a range from Fermi-level to −4.6 eV is occupied by O-2p states, while above Fermi level, Pa-4f states contribute to the formation of first conduction band. As a whole, the conduction band is due to the fact that states of X:3d are mixed with Pa:d for $XPaO_3$ structure.

Electron density plots can be used to evaluate the bonding nature in crystalline solid.[57] The charge densities for $XPaO_3$ (K, Rb) are calculated along (100) and (110) planes in three dimensions (3D) as shown in Fig. 4. The density contour in the (110) direction indicates that the bonding between X–O ions is ionic, because much less overlapping is seen between X and O ions. However, bonding between Pa–O ions is strongly covalent as large sharing is observed. In fact, the covalent nature is due to pd-hybridization between cations and anions.

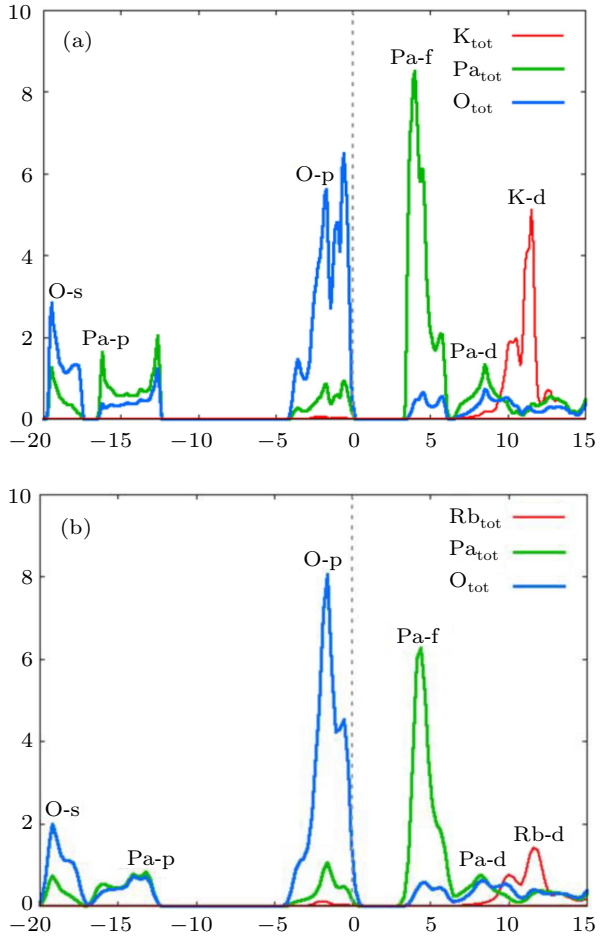


Fig. 3. (color online) Calculated values of total and partial density of states (TDOS & PDOS) of (a) $KPaO_3$ and (b) $RbPaO_3$.

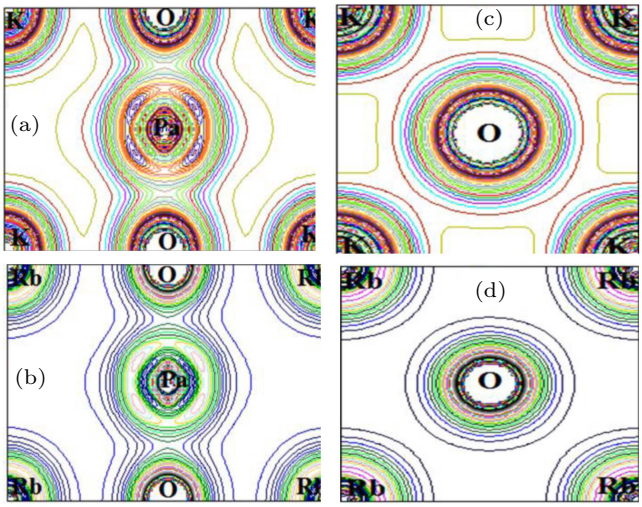


Fig. 4. (color online) Calculated mBJ total three-dimensional electronic charge densities. (a) $KPaO_3$ in (110) plane, (b) $RbPaO_3$ in (110) plane, (c) $KPaO_3$ in (100) plane, (d) $RbPaO_3$ in (100) plane.

Table 5. Band gap comparison of $X\mathrm{PaO_3}$ (X = K, Rb) at different symmetry points.

Compound	Symmetry point	Bandgap type	E_g^{MBJ}/eV	E_g^{LDA}/eV	$E_g^{\mathrm{WC\text{-}GGA}}$/eV	$E_g^{\mathrm{PBE\text{-}GGA}}$/eV	$E_g^{\mathrm{Pbsol\text{-}GGA}}$/eV
$\mathrm{KPaO_3}$	Γ–Γ	direct	3.60	3.41	3.51	3.49	3.45
	R–R	indirect	4.41	4.22	4.33	4.31	4.27
	M–M	indirect	4.45	4.32	4.42	4.39	4.36
	X–X	indirect	4.39	4.21	4.31	4.29	4.26
$\mathrm{RbPaO_3}$	Γ–Γ	direct	3.14	2.93	3.04	3.01	2.97
	R–R	indirect	3.38	3.27	3.34	3.31	3.29
	M–M	indirect	3.42	3.21	3.39	3.37	3.23
	X–X	indirect	3.21	2.98	3.18	3.12	3.10

3.5. Optical properties

In this subsection, the optical properties of $X\mathrm{PaO_3}$ compounds are investigated by means of the Trans–Blaha modified Becke–Johnson (TB-mBJ) potential. Fundamental optical responses include the imaginary part of dielectric function $\varepsilon_2(\omega)$, the real part of dielectric function $\varepsilon_1(\omega)$, extinction coefficient $k(w)$, absorption coefficient $\alpha(\omega)$, reflectivity $R(\omega)$, optical conductivity $\sigma(\omega)$, energy loss function $L(\omega)$, and effective number of electrons n_{eff} via sum rules. The complex dielectric function $\varepsilon(\omega)$ can break into real and imaginary parts according to the following relation:[58]

$$\varepsilon(\omega) = \varepsilon_1(\omega) + \mathrm{i}\varepsilon_2(\omega). \tag{14}$$

In Eq. (14) $\varepsilon_2(\omega)$ denotes the imaginary part of dielectric function while $\varepsilon_1(\omega)$ represents the real part dielectric function. The analysis of $\varepsilon_2(\omega)$ gives complete response of material due to applied electromagnetic radiation as shown in Fig. 5. The imaginary part of dielectric function can be expressed by the following equation:[59]

$$\varepsilon_2(\omega) = \left(\frac{4\pi^2 e^2}{m^2\omega^2}\right) \times \sum_{i,j}\int_k \langle \mathrm{i}|M|j\rangle^2 f_i(1-f_i)\,\delta\left(E_{j,k}-E_{i,k}-\omega\right)\mathrm{d}^3k. \tag{15}$$

In Eq. (15) M is the dipole matrix, f_i is the i-th state Fermi distribution function, $E_{i,k}$ and $E_{j,k}$ are the i-th and j-th state energies of electron in crystal wave vector k, respectively. The widespread peaks of $\varepsilon_2(\omega)$ follow the pattern of density of states (DOS) and the band structure of the investigated compound. The threshold energy points occur approximately at 3.81 eV and 3.99 eV for $\mathrm{KPaO_3}$ and $\mathrm{RbPaO_3}$ respectively, while the major peaks are located at 6.1 eV and 6.3 eV, which correspond to transition of occupied valence band states to unoccupied conduction band states. These peaks are majorly due to Pa-4f states. After that the diverse peaks are observed till 15 eV which occurs due to hybridized states of X-3d along with some p and d states of Pa as well as O respectively. The phenomenon of polarization is observed with the help of the real part of dielectric function $\varepsilon_1(\omega)$ as shown in Fig. 6. It can be expressed via the following equation:[60]

$$\varepsilon_1(\omega) = 1 + \frac{2}{\pi}\mathrm{P}\int_0^{\varphi}\frac{\omega'\varepsilon_2(\omega')\,\mathrm{d}\omega'}{\omega'^2-\omega'^2}, \tag{16}$$

where P is the principle value of the corresponding integral. At zero frequency limit the static parts of dielectric function $\varepsilon_1(0)$ are observed at 4.31 eV and 3.89 eV for $\mathrm{KPaO_3}$ and $\mathrm{RbPaO_3}$ respectively.

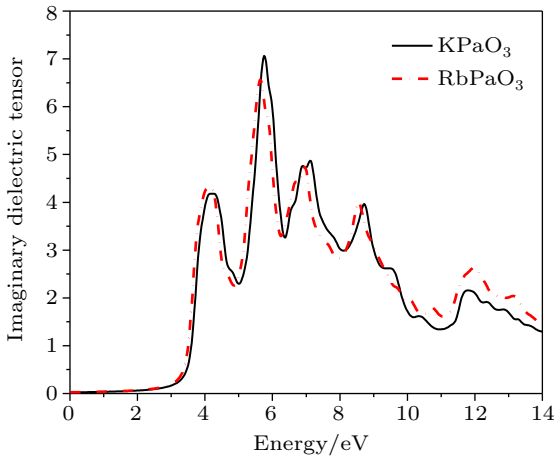


Fig. 5. (color online) Calculated imaginary part $\varepsilon_2(\omega)$ of the dielectric function.

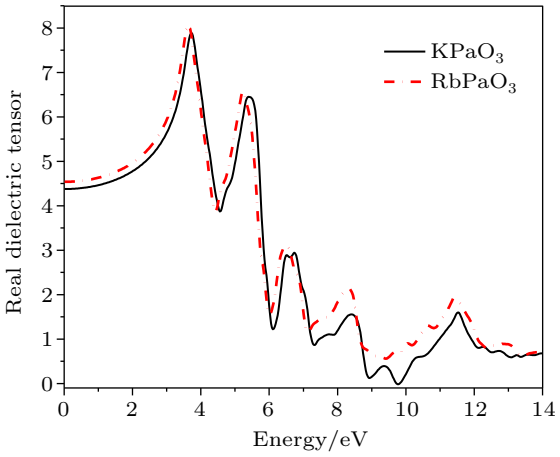


Fig. 6. (color online) Calculated real part $\varepsilon_1(\omega)$ of the dielectric function for $X\mathrm{PaO_3}$ (K, Rb) compounds for $X\mathrm{PaO_3}$ (K, Rb) compounds.

The curves of $\varepsilon_1(\omega)$ start to increase and attain their maximum values approximately at 3.7 eV for $X\mathrm{PaO_3}$ (X = K, Rb) compounds. The calculated values of the optical conductivity

$\sigma(\omega)$ for XPaO$_3$ (X = K, Rb) compounds are shown in the following Fig. 7.

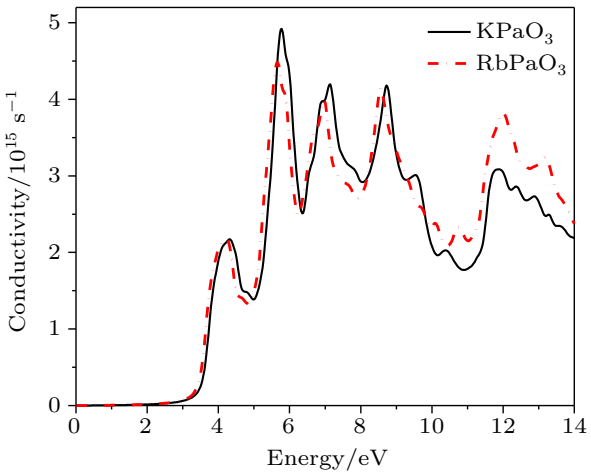


Fig. 7. (color online) Calculated conductivity $\sigma(\omega)$ for XPaO$_3$ (K, Rb) compounds.

The journeys of optical conductivity start at about 2 eV from small ascending peak and then eventually reach their distinct maxima at about 5.8 eV for both compounds. It is evident from the above analysis that the spectrum of optical conductivity shifts towards low energy ranges from Rb to K due to small bandgaps of the compounds. The spectrum of electron energy loss function $L(\omega)$ depicts the characteristic contribution associated with plasma resonance frequency (ω_p)[61] as shown in Fig. 8. A distinct sharp peak of electron energy loss is observed approximately at 10.0 eV.

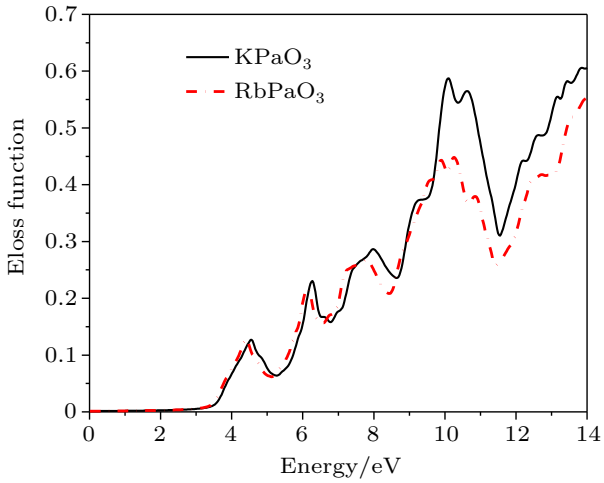


Fig. 8. (color online) Calculated energy loss function $L(\omega)$ for XPaO$_3$ (K, Rb) compounds.

The calculated spectra of refractive index and reflectivity as a function of electromagnetic energy are shown in Figs. 9 and 10. The static parts of refractive index $n(0)$ represent important quantities which are 2.07 and 2.09 for KPaO$_3$ and RbPaO$_3$ respectively. The curves of refractive index reach their maximum values of 2.81 at 4 eV for KPaO$_3$ and 2.82 at 4.1 eV for RbPaO$_3$, respectively. Furthermore XPaO$_3$ (X = K, Rb) compound starts to reflect highly and attains maximum values in a range of 21 eV–25 eV. Hence, these materials show that they are transparent in this particular energy range.

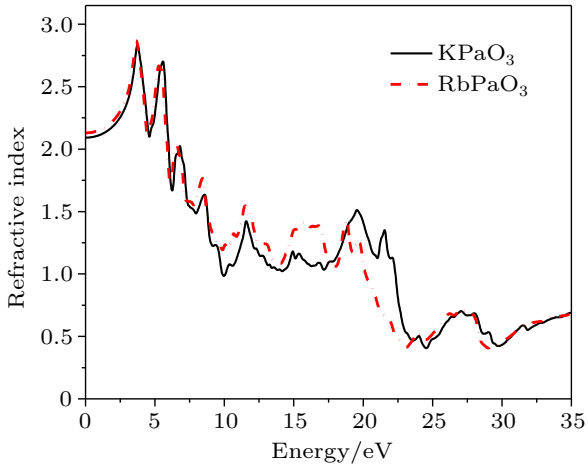


Fig. 9. (color online) Refractive index $n(\omega)$ as a function of energy for XPaO$_3$ (X = K, Rb) compounds.

The plots of absorption coefficient as a function of energy depict that compounds start to absorb the electromagnetic radiation at about 4.25 eV as indicated in Fig. 11. This particular energy (threshold point) is exactly in accordance with trend of bandgap. However, these compounds start to absorb effectively in a range of 21 eV–25 eV while the highest prominent peak is observed at around 23 eV. After the optimum absorption peak, it again decreases and suffers trivial variations. The analyses of absorption spectra indicate clearly the applications of these oxide perovskites for absorption purposes in wide ultra-violet region, typically at about 23 eV. Next, the sum rule is used to evaluate the effective number of valence electrons per unit cell that are engaged in intra-band as well as inter-band transitions.[62] It can be observed from Fig. 12 that inter-band transition of electrons occurs around 3.5 eV. The trend-line increases slowly but there occurs a sharp peak showing an abrupt increase of electrons which saturates in a range of 12 eV–14 eV.

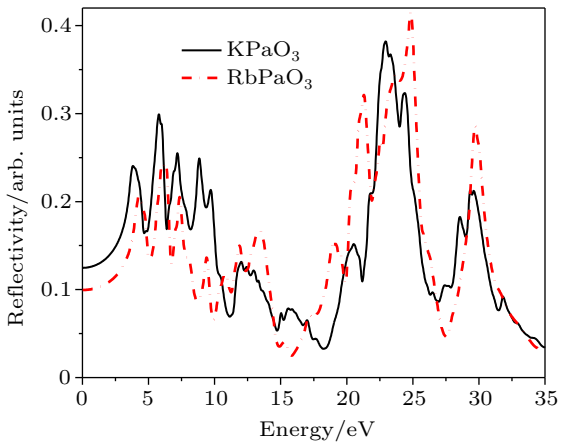


Fig. 10. (color online) Reflectivity $R(\omega)$ as a function of energy for XPaO$_3$ (X = K, Rb) compounds.

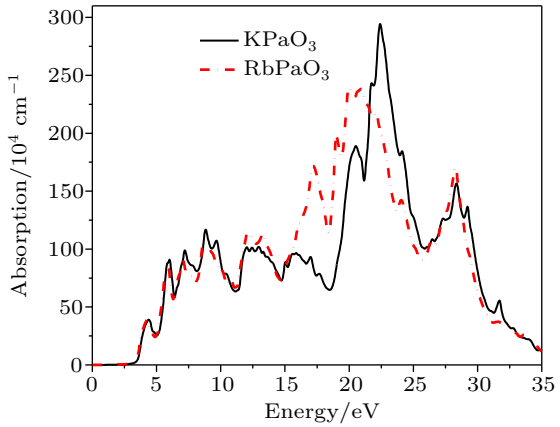


Fig. 11. (color online) Absorption coefficient $\alpha(\omega)$ as a function of energy for XPaO$_3$ (K, Rb) compounds.

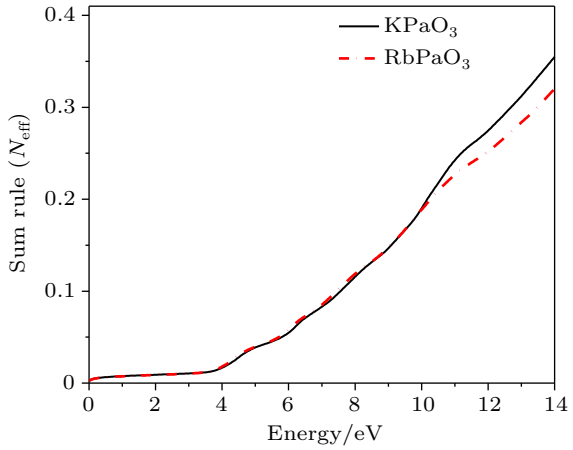


Fig. 12. (color online) Calculated sum rule ($N_{\rm eff}$) for XPaO$_3$ (X = K, Rb) compounds.

4. Conclusions

In this work, all electron self-consistent full potential-linearized augmented plane wave (FP-LAPW) method is used to explore structural, electronic, mechanical, and optical properties of XPaO$_3$ (X = K, Rb) within generalized gradient approximation (GGA), local density approximation (LDA), and Trans–Blaha modified Becke–Johnson (TB-mBJ) potential. Structural properties are also evaluated by analytical techniques. Energy band profile confirms that the investigated materials are (Γ–Γ) direct bandgap semiconductors. The curves of total and partial density of states are used to determine the contribution of different bands. The detailed analyses of elastic and mechanical parameters prove flexible, anisotropic, and covalent nature of the herein compounds. These results are in favorable agreement with previous theoretical and existing experimental data. The optical properties are discussed in terms of complex dielectric function $\varepsilon(\omega)$ and the analysis is carried out by interband contribution that shows that the XPaO$_3$ (X = K, Rb) compounds possess wide ranges of absorption and reflection in high frequency regions and these characteristics make them useful for flexible opto–electronic applications. In summary, these perovskites are efficiently employed in scientific investigation and need an extensive experimental research for their possible technological benefit.

References

[1] Tezuka K and Hinatsu Y 2001 *J. Solid State Chem.* **156** 203
[2] Li L Q, Kennedy B J, Kubota Y, Kato K and Garrett R F 2004 *J. Mater. Chem.* **14** 263
[3] Maekawa T, Kurosaki K and Yamanaka S 2006 *J. Alloys Compd.* **407** 44
[4] Lupina G, Kozlowski G, Dąbrowski J, Wenger C, Dudek P, Zaumseil P, Lippert G, Walczyk C and Müssig H J 2008 *Appl. Phys. Lett.* **92** 062906
[5] Kukli K, Ritala M, Sajavaara T, Hanninen T and Leskela M 2006 *Thin Solid Films* **500** 322
[6] Fursenko O, Bauer J, Lupina G, Dudek P, Lukosius M, Walczyk C and Zaumseil P 2012 *Thin Solid Films* **520** 4532
[7] Dotzler C, Williams G V M and Edgar A 2008 *Curr. Appl. Phys.* **8** 447
[8] Bayindir M, Sorin F, Abouraddy A F, Viens J, Hart S D, Joannopoulos J D and Fink Y 2004 *Nature* **431** 826
[9] Campbell P K, Jones K E, Huber R J, Horch K W and Normann R A 1991 *IEEE Trans. Biomed. Eng.* **38** 758
[10] Kim D H, Wiler J A, Anderson D J, Kipke D R and Martin D C 2010 *Acta Biomaterialia* **6** 57
[11] Nilsen O, Rauwel E, Fjellvag H and Kjekshus A 2007 *J. Mater. Chem.* **17** 1466
[12] Aaltonen T, Alnes M, Nilsen O, Costelle L and Fjellvag H 2010 *J. Mater. Chem.* **20** 2877
[13] Cuevas-Saavedraa R and Staroverov V N 2016 *Mol. Phys.* **114** 1050
[14] Hohenberg P and Kohn W 1964 *Phys. Rev. B* **136** 864
[15] Bentouaf A and Hassan F H 2015 *J. Magn. Magn. Mater.* **381** 65
[16] Abbassi A, Arejdal M, Ez-Zahraouy H and Benyoussef A 2016 *Opt. Quantum Electron.* **48** 38
[17] Iyer P N and Smith A J 1967 *Acta Cryst.* **23** 740
[18] Blaha P, Schwarz K, Sorantin P and Trickey S B 1990 *Comput. Phys. Commun.* **59** 399
[19] Kohn W and Sham L J 1965 *Phys. Rev.* **140** 1133
[20] Tran F and Blaha P 2009 *Phys. Rev. Lett.* **102** 226401
[21] Koelling D D and Harmon B N 1977 *J. Phys. C: Solid State Phys.* **10** 3107
[22] Murnaghan F D 1944 *Proc. Natl. Acad. Sci. USA* **30** 244
[23] Muller O and Roy R 1974 *The Major Ternary Structural Families* (NewYork-Heidelberg-Berlin: Springer)
[24] Morss L R, Edelstein N M, Katz J J 2006 *The chemistry of the actinide and transactinide elements* (Springer)
[25] Jain A, Ong S P, Hautier G, Chen W, Richards W D, Dacek S, Cholia S, Gunter D, Skinner D, Ceder G and Persson K A 2013 *The Materials Project: A materials genome approach to accelerating materials innovation* APL Materials 1(1), 011002
[26] Majid A and Lee Y S 2010 *Adv. Inform. Sci. Serv. Sci.* **2** 118 (ISSN:1976-3700)
[27] Verma A S, Kumar A, Bhardwaj S R 2008 *Phys. Status Solidi B* **245** 1520
[28] Jiang L Q, Guo J K, Liu H B, Zhu M, Zhou X, Wu P and Li C H 2006 *J. Phys. Chem. Solids* **67** 1531
[29] Moreira R L and Dias A 2007 *J. Phys. Chem. Solids* **68** 1617
[30] Clementi E, Raimondi D L and Reinhardt W P 1963 *J. Chem. Phys.* **38** 2686
[31] Ali Z, Khan I, Ahmad I, Khan M S and Asadabadi S J 2015 *Mat. Chem. Phys.* **162** 308
[32] Goldschmidt V M 1958 *Geochemistry* (UK: Oxford University Press)
[33] Catalan G and Scott J F 2009 *Adv. Mater.* **21** 2463
[34] Ghebouli B, Ghebouli M A, Bouhemadou A, Fatmi M, Khenata R, Rached D, Ouahrani T and Omran S B 2012 *Solid State Sci.* **14** 903
[35] Chen B A, Liu G, Wang R H, Zhang J Y, Jiang L, Song J J and Sun J 2013 *Acta Mater.* **61** 1676
[36] Goodenough J B 2004 *Rep. Prog. Phys.* **67** 1915
[37] Xu N, Zhao H, Zhou X, Wei W, Lu X, Ding W and Li F 2010 *J. Hydrog. Energy* **35** 7295
[38] Holm B, Ahuja R, Yourdshahyan Y, Johanson B and Lundqvist B I 1999 *Phys. Rev. B* **59** 12777

[39] Mase G T and Mase G E 1999 *Elasticity: Theory, Applications, and Numerics*, 2nd edn. (New York: CRC Press LLC)
[40] Meziani A and Belkhir H 2012 *Comput. Mater. Sci.* **61** 67
[41] Erum N and Iqbal M A 2016 *Commun. Theor. Phys.* **66** 571
[42] Hill R 1952 *Proc. Phys. Soc. Lond. A* **65** 349
[43] Dong S and Liu J M 2012 *Mod. Phys. Lett. B* **26** 1230004
[44] Sadd M H 2005 *Elasticity Theory, Applications, and Numerics Elsevier* (UK: Academic Press)
[45] Voigt W 1889 *Ann. Phys. (Germany)* **38** 573
[46] Pugh S F 1954 *Philos. Mag.* **45** 823
[47] Brik M G 2010 *J. Phys. Chem. Solids* **71** 1435
[48] Pettifor D G 1992 *Mater. Sci. Technol.* **8** 345
[49] Callaway J 1991 *Quantum Theory of the Solid State*, 2nd edn. (New York: Academic Press)
[50] Frantsevich I N, Voronov F F and Bokuta S A 1983 *Elastic constants and elastic moduli of metals and insulators handbook* (Kiev: Naukova Dumka) pp. 60–180
[51] Yildirim A, Koc H and Deligoz E 2012 *Chin. Phys. B* **21** 037101
[52] Haines J, Léger J M and Bocquillon G 2001 *Ann. Rev. Mater. Res.* **31** 1
[53] Jamal M, Abu-Jafar M S and Reshak A H 2016 *J. Alloys Compd.* **667** 151
[54] Fine M E, Brown L D and Marcus H L 1984 *Scripta Metall.* **18** 951
[55] Saini H S, Singh M, Reshak A H and Kashyap M K 2012 *J. Alloys Compd.* **518** 74
[56] Cuevas-Saavedraa R and Staroverov V N 2016 *Mol. Phys.* **114** 1050
[57] Hoffman R 1988 *Rev. Mod. Phys.* **60** 601
[58] Fox M 2001 *Optical Properties of Solids* (New York: Oxford University Press)
[59] Wooten F 1972 *Optical Properties of Solids* (New York: Academic Press)
[60] Abelès F, 1972 *Optical Properties of Solids* (Amsterdam/New York: North-Holland Pub. Co., American Elsevier)
[61] Kumar S, Maury T K and Auluck S 2008 *J. Phys: Condens. Matter* **20** 075205
[62] Slack G A 1973 *J. Phys. Chem. Solids* **34** 321